NANO LETTERS

Letter

pubs.acs.org/NanoLett

Molecular Packing and Solar Cell Performance in Blends of Polymers with a Bisadduct Fullerene

Nichole Cates Miller,[†] Sean Sweetnam,[†] Eric T. Hoke,[†,‡] Roman Gysel,[†] Chad E. Miller,[†,§] Jonathan A. Bartelt,[†] Xinxin Xie,[†] Michael F. Toney,[§] and Michael D. McGehee*[,†]

[†]Department of Materials Science and Engineering and [‡]Department of Applied Physics, Stanford University, Stanford, California 94305, United States

[§]Stanford Synchrotron Radiation Lightsource, SLAC National Accelerator Laboratory, Menlo Park, California 94025, United States

Supporting Information

ABSTRACT: We compare the solar cell performance of several polymers with the conventional electron acceptor phenyl-C61-butyric acid methyl ester (PCBM) to fullerenes with one to three indene adducts. We find that the multiadduct fullerenes with lower electron affinity improve the efficiency of the solar cells only when they do not intercalate between the polymer side chains. When they intercalate between the side chains, the multiadduct fullerenes substantially reduce solar cell photocurrent. We use X-ray diffraction to determine how the fullerenes are arranged within crystals of poly-(2,5-bis(3-tetradecylthiophen-2-yl)thieno[3,2-b]thiophene) (PBTTT) and suggest that poor electron transport in the molecularly mixed domains may account for the reduced solar cell performance of blends with fullerene intercalation.

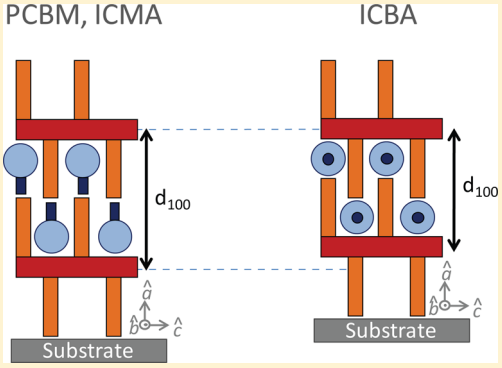

KEYWORDS: *Organic materials, solar cells, X-ray diffraction, molecular packing*

Bulk heterojunction (BHJ) organic solar cells based on blends of a conjugated polymer (donor) and a fullerene derivative (acceptor) are promising as an inexpensive, flexible, and printable alternative to traditional silicon solar cells.[1−3] Fullerene bisadducts have attracted attention as promising electron-accepting materials because of their ability to increase the open-circuit voltage (V_{OC}) of organic solar cells due to their relatively high lowest unoccupied molecular orbital (LUMO) energy levels compared to the widely used phenyl-C61-butyric acid methyl ester (PCBM).[4−9] Indene-C60 bisadduct (ICBA), for example, improves the efficiency of poly(3-hexylthiophene) (P3HT) solar cells from ∼4% to 6.5% due to an increase in the V_{OC} when it replaces PCBM as the electron acceptor (see Figure 1 for the chemical structures).[10−12] Surprisingly, ICBA does not perform well when it is blended with most other polymers.[13] Here, we compare the solar cell performance of a variety of polymer:PCBM and polymer:ICBA blends. We also determine the molecular packing motif of polymer blends with indene-C60 fullerenes with one (ICMA), two (ICBA), and three (ICTA) indene side groups and use this knowledge to suggest an explanation for why ICBA outperforms PCBM as the electron acceptor in some BHJ solar cells but not in others.

We first determine the solar cell performance of polymer blends with PCBM and ICBA. All solar cells were spin cast from *ortho*-dichlorobenzene (DCB) onto poly(3,4-ethylenedioxythiophene):poly(styrenesulfonate) (PEDOT:PSS, Baytron)-covered indium tin oxide (ITO)-coated glass substrates (Xin Yang Technology). Ca/Al electrodes were then evaporated. In agreement with previous results,[10−12] the P3HT:ICBA solar cells outperformed P3HT:PCBM devices due to an increase in the V_{OC} (Table 1). Similar efficiency increases were observed for blends with the conjugated polymers poly(2,5-bis(3-2,7-dimethyloctylthiophen-2-yl)-thieno[3,2-b]thiophene) (PBTTT-branched) and poly(3,6-dialkylthieno[3,2-*b*]thiophene-*co*-bithiophene) (PATBT). For all three of these polymers, replacing PCBM with ICBA results in an increased efficiency, fill factor (FF), and V_{OC}. On the other hand, replacing PCBM with ICBA decreases the performance of solar cells based on the conjugated polymers poly(*N*-9″-hepta-decanyl-2,7-carbazole-*alt*-5,5-(4′,7′-di-2-thienyl-2′,1′,3′-benzothiadiazole)) (PCDTBT), poly(2,3-bis-(3-octyloxyphenyl)quinoxaline-5,8-diyl-*alt*-thiophene-2,5-diyl) (PTQ1), and poly-(2,5-bis(3-tetradecylthiophen-2-yl)thieno-[3,2-b]thiophene) (PBTTT), which is the same as PBTTT-branched except that it has linear side chains. These efficiency decreases are due to large decreases in the FF and short-circuit current (J_{SC}).

To determine why ICBA outperforms PCBM in blends with P3HT, PBTTT-branched, and PATBT, while PCBM outperforms ICBA in blends with PBTTT, PCDTBT, and PTQ1, we characterized the molecular packing in the films. Previous studies have shown that fullerenes can intercalate between the

Received: December 14, 2011
Revised: February 23, 2012
Published: February 29, 2012

 © 2012 American Chemical Society dx.doi.org/10.1021/nl204421p | *Nano Lett.* 2012, 12, 1566−1570

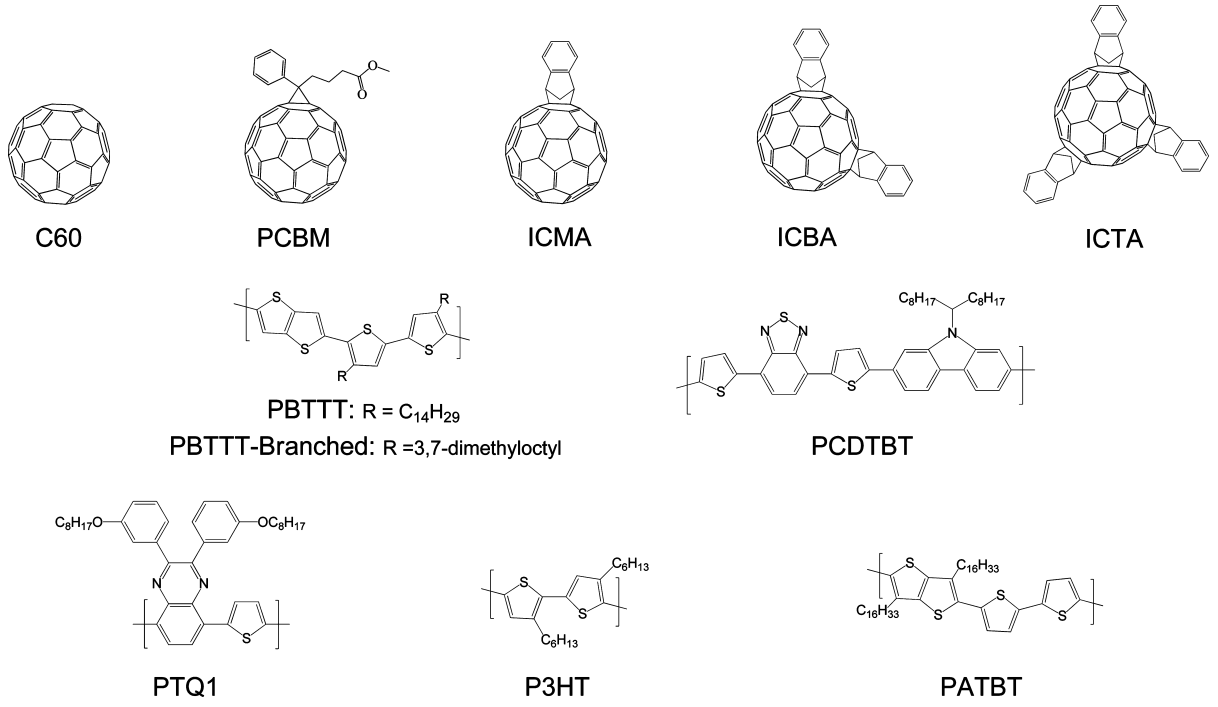

Figure 1. Chemical structures of the materials discussed in this paper.

Table 1. Solar Cell Parameters for the Highest Efficiency Polymer:PCBM and Polymer:ICBA Solar Cells Made in Our Lab[a]

polymer	fullerene	polymer:fullerene wt ratio	intercalation	eff. (%)	FF	J_{SC} (mA/cm^2)	V_{OC} (V)
PBTTT	PCBM	1:4	yes[14,15]	*2.25*	0.61	7.02	0.526
	ICBA	1:4	yes	1.21	0.52	3.63	0.636
PCDTBT	PCBM	1:4	yes[20]	*3.61*	0.56	7.54	0.856
	ICBA	1:4	yes	1.68	0.44	3.57	1.063
PTQ1	PCBM	1:3	probably[b]	3.40	0.66	5.92	0.875
	ICBA	1:3	probably	1.36	0.49	2.74	1.019
P3HT	PCBM	1:1	no[14]	4.25	0.67	10.0	0.635
	ICBA	1:1	no	*5.95*	0.70	10.0	0.850
PBTTT-branched	PCBM	1:1	no	1.14	0.50	3.94	0.575
	ICBA	1:1	no	*1.82*	0.54	4.48	0.755
PATBT	PCBM	1:1	no	1.79	0.56	5.47	0.582
	ICBA	1:1	no	*1.84*	0.62	3.40	0.871

[a]The highest efficiency blend from each pair is in italics. Polymer:ICMA solar cell performances are not shown because the limited solubility of ICMA results in optically thin, inefficient devices. [b]Based on optimal polymer:fullerene ratio.

side chains of many conjugated polymers, including PBTTT[14−19] and PCDTBT,[20] to form mixed polymer:fullerene phases.[21−23] However, fullerenes do not intercalate in crystalline domains of P3HT, PBTTT-branched, and PATBT.[14,18,24] Thus, the blends without fullerene intercalation exhibit efficiency increases when ICBA replaces PCBM, whereas the blends with intercalation show significantly reduced photocurrent production. Below, we use specular X-ray diffraction (XRD) to determine the molecular packing motif of blends with ICMA, ICBA, and ICTA and demonstrate that the observed decrease in the solar cell performance of intercalated blends with ICBA may be explained by a difference in the ability of electrons to escape the intercalated polymer:-fullerene phases.

Figure 2 shows the specular XRD patterns of PBTTT blends with ICMA, ICBA, and ICTA. The XRD patterns for PBTTT:PCBM, PBTTT:C60, and pure PBTTT are shown for comparison. All XRD samples except for PBTTT:C60 were prepared by spin coating from DCB onto silicon substrates. The PBTTT:C60 film was prepared as described in ref 17. Specular XRD measurements were performed with a X-ray energy of 8 keV at beamline 2-1 at the Stanford Synchrotron Radiation Lightsource. These XRD patterns show that the lamellar spacing of pure PBTTT (21.5 Å) increases to 28.5, 26.0, and 23.1 Å for PBTTT blends with ICMA, ICBA, and ICTA, respectively. This trend was surprising, because the larger fullerenes resulted in smaller lamellar spacings. The lamellar spacing for PBTTT:ICTA is close to that of pure PBTTT (Figure 2), because ICTA is too bulky to intercalate between the PBTTT side chains; thus the PBTTT:ICTA blend phase separates into relatively pure PBTTT and pure ICTA domains. The absence of intercalation in PBTTT:ICTA blends is also evident from the absence of an in-plane peak at q_{xy} = 0.49 Å^{-1} in the two-dimensional grazing incidence X-ray scattering (2D GIXS) pattern (Figure S1, Supporting Information). This peak, which only occurs in intercalated blends, is due to the ordering of the fullerene in the bimolecular crystal along the *c*-axis.[14,17] Both PBTTT:ICMA and

dx.doi.org/10.1021/nl204421p | *Nano Lett.* 2012, 12, 1566−1570

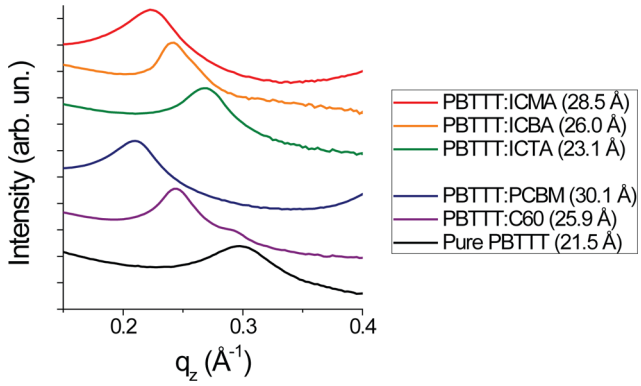

Figure 2. Specular XRD patterns for PBTTT blends with ICMA (red), ICBA (orange), ICTA (green), PCBM (blue), and C60 (purple) as well as pure PBTTT (black). All blends have a 1:1 PBTTT:fullerene molar ratio except for the PBTTT:C60 blend, for which the precise blend ratio is unknown due to the preparation conditions. The lamellar spacings for the samples are given in the legend.

PBTTT:ICBA exhibit this peak at q_{xy} = 0.49 Å, indicating that intercalation occurs in these blends. It is still surprising that the larger ICBA fullerene results in a smaller lamellar spacing than ICMA when it is blended with PBTTT; we will show that this difference is due to the different orientations of the fullerenes in PBTTT:ICMA and PBTTT:ICBA blends.

The specular XRD and 2D GIXS patterns of PBTTT:ICMA and PBTTT:PCBM are very similar, indicating that these blends have similar molecular packing. For example, the lamellar spacing of PBTTT:ICMA (28.5 Å) is similar to that of PBTTT:PCBM (30.1 Å), as shown in Figure 2, and the specular XRD intensities, particularly the abnormally strong *(700)* peak, are similar for these two blends (Figure 3).

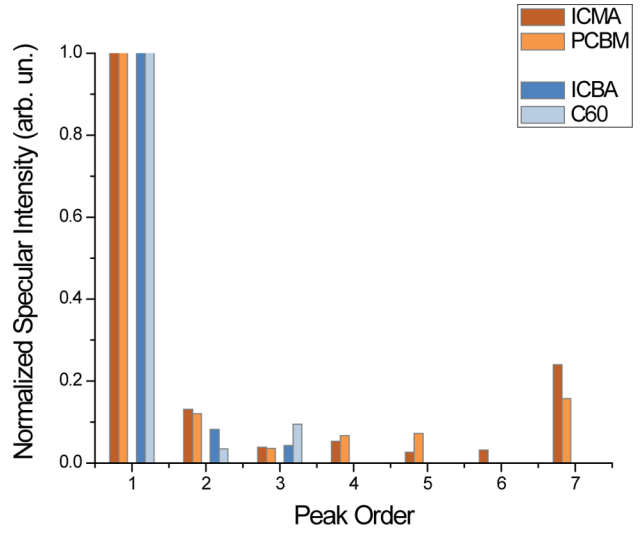

Figure 3. Normalized experimental specular XRD intensities for the PBTTT blends with ICMA (dark brown), PCBM (light brown), ICBA (dark blue), and C60 (light blue) corrected as described in ref 17.

Although the origin of the intense (700) peak is not fully understood, it appears to be related to the distance between the polymer backbone and the intercalated fullerene. The in-plane diffraction peaks of the 2D GIXS patterns (those near q_z = 0 along the q_{xy} axis) for PBTTT:ICMA and PBTTT:PCBM also have similar positions (Figure S1, Supporting Information).

The PCBM side group has been shown to be on average parallel to the polymer side chains (perpendicular to the substrate) in the PBTTT:PCBM bimolecular crystal, as illustrated in Figure 4A.[17] The PCBM side group therefore

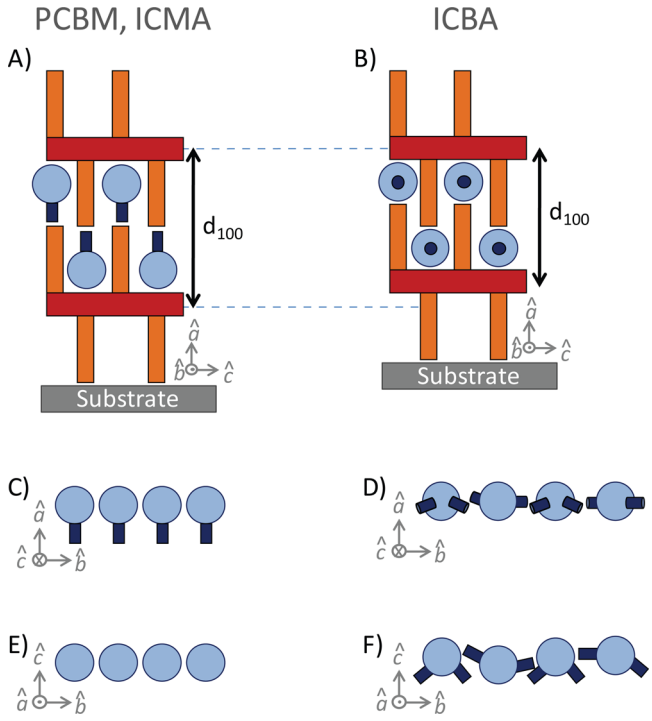

Figure 4. Illustrations of the molecular packing viewed along the *b*-axis (A,B) and the fullerene channels viewed along the *c*-axis (C,D) and *a*-axis (E,F) in PBTTT blends with PCBM and ICMA (A,C,E) and ICBA (B,D,F). The polymer backbones, polymer side chains, fullerene cages, and fullerene side groups are colored red, orange, light blue, and dark blue, respectively. These are simplified illustrations meant to show the likely relative locations and do not depict the precise packing of the bimolecular crystal or the exact ICBA isomeric structures.

contributes to the lamellar spacing of the PBTTT:PCBM bimolecular crystal. Due to the similarities between the specular XRD and 2D GIXS patterns of the PBTTT blends with ICMA and PCBM, it is likely that the ICMA side group is also parallel to the PBTTT side chains, as illustrated in Figure 4A.

On the other hand, the specular XRD and 2D GIXS patterns of PBTTT:ICBA and PBTTT:C60 show many similarities. For instance, the lamellar spacing of PBTTT:ICBA (26.0 Å) is very similar to that of PBTTT:C60 (25.9 Å) (Figure 2). The specular XRD intensities of these two blends are also similar, with neither of these blends exhibiting a strong (700) peak as was observed for the ICMA and PCBM blends (Figure 3). In addition, there are many similarities in the 2D GIXS patterns of these two blends, such as the lack of a peak at q_{xy} = 0.67 Å^{-1} (Figure S1, Supporting Information). We therefore conclude that the molecular packing of PBTTT:ICBA is similar to that of PBTTT:C60 and that ICBA's two side groups probably lie nearly parallel to the plane of the substrate (largely perpendicular to the PBTTT side chains), as illustrated in Figure 4B. As a result, ICBA's side groups do not contribute to the lamellar spacing of the PBTTT:ICBA bimolecular crystal, which explains why PBTTT:ICBA and PBTTT:C60 have nearly identical lamellar spacings.

One of the likely reasons that the ICBA side groups orient parallel to the substrate is to allow the conjugated polymer

dx.doi.org/10.1021/nl204421p | *Nano Lett.* 2012, 12, 1566–1570

backbone to interact with the conjugated fullerene cage. For the ICBA isomers that have indene side groups on approximately opposite sides of the fullerene cage, this interaction would not be possible if the indene side groups were perpendicular to the substrate. In the most common ICBA isomer, the two indene side groups are separated by ~90°.[25] This ICBA isomer can fit into the bimolecular crystal with its side groups parallel to the substrate by having the indene side groups penetrate into the region occupied by the polymer side chains, as illustrated in Figure S3, Supporting Information. In a separate manuscript, we provide solid-state nuclear magnetic resonance (NMR) and Fourier transform infrared spectroscopy (FTIR) data to show that the PBTTT side chains are largely amorphous in the bimolecular crystal, thus making it possible for the indene side groups to penetrate the PBTTT side chains.[17] Another likely reason that ICBA orients with its side groups in the substrate plane is that it allows for a more orderly and dense packing structure that accommodates the mixture of ICBA isomers. If one or both of the ICBA side groups were to orient perpendicular to substrate, different isomers would locally increase the lamellar spacing by different amounts due to the different dimensions of the isomers. The resulting disorder would be energetically unfavorable.

The different orientations of PCBM and ICBA may affect the ability of the fullerene channels to conduct electrons through the PBTTT:fullerene bimolecular crystals. Figure 4 shows illustrations of the fullerene channels in PBTTT:PCBM and PBTTT:ICBA bimolecular crystals. Previously performed density functional theory calculations[17] and time-resolved microwave conductivity (TRMC) measurements[26] have shown that electrons can travel along the fullerene channels in PBTTT:PCBM bimolecular crystals to reach pure PCBM domains. However, electron transport through the fullerene channels in the PBTTT:ICBA bimolecular crystal may be partially blocked by the presence of nonconjugated indene side groups. When fullerenes intercalate between polymer side chains, four transport directions are blocked by the polymer side chains and the polymer backbones. If the remaining two directions are completely or partially blocked by fullerene side groups, then there will be no good pathway for electron transport through the bimolecular crystal. This may explain why ICBA does not perform as well as PCBM in intercalated blends even though it improves the performance of blends without intercalation.

Poor electron transport through mixed polymer:fullerene domains may also explain the poor performance of multiadduct fullerenes in blends with amorphous polymers. For the reasons discussed above, a bisadduct fullerene intercalated between the side chains of an amorphous polymer is likely to orient in such a way that its side groups lie in the plane roughly perpendicular to the polymer side chains. Amorphous polymers may therefore suffer from poor electron transport through mixed polymer:-fullerene domains due to blockage of electron transport by the polymer backbones, the polymer side chains, and the fullerene side groups in a manner similar to that described above for bimolecular crystals. This could explain why the space-charge limited current electron mobility was found to be 2 orders of magnitude lower in blends of a low bandgap polymer with the multiadduct fullerene bisPCBM than in films of the pure fullerene.[27]

Other factors could also explain the inferior performance of ICBA relative to PCBM in intercalated blends. For instance, Durrant et al. recently demonstrated using cyclic voltammetry that electrons in PCBM clusters are more stable than electrons on isolated PCBM molecules, giving rise to a driving force for electrons to escape molecularly mixed phases and reach pure PCBM domains.[28] They show that this driving force does not exist in blends with a branched adduct fullerene derivative, 1,1-bis(4,4′-dodecyloxyphenyl)-(5,6) C_{61} (DPM-12),[29] and speculate that this driving force also does not exist in blends with ICBA due to inhibited agglomeration from its multiple adducts.

Energetic considerations may provide an additional cause for reduced photocurrent in some ICBA devices. The higher lying highest occupied molecular orbital (HOMO) and LUMO energies of ICBA compared to PCBM results in a smaller free-energy driving force for charge transfer from singlet and triplet excitons on the polymer and fullerene, which has been shown to correlate with a reduced charge generation yield[30,31] and may also allow geminate electron−hole pairs to recombine exergonicly into triplet excitons on the polymer or fullerene.[32] These energetic considerations, however, cannot explain why PBTTT-branched and PATBT perform better with ICBA, while PBTTT performs better with PCBM (see Supporting Information). It is likely that suboptimal energy levels for charge generation and an intercalated morphology with poor transport through the fullerene channels are two problems that can occur independently in ICBA devices.

In conclusion, we have compared the solar cell performance and molecular packing motif of polymer blends with the fullerene acceptors ICBA and PCBM. We find that ICBA can outperform PCBM in nonintercalated blends, whereas PCBM consistently outperforms ICBA in blends with intercalation. Furthermore, we show that the intercalated fullerenes in PBTTT:ICBA bimolecular crystals orient with their side groups parallel to the substrate. This fullerene orientation could cause poor electron transport through the fullerene channels in the bimolecular crystal, since nonconjugated fullerene side groups separate the conjugated fullerene cages. Like PBTTT:ICBA blends, other intercalated polymer:fullerene bisadduct blends probably also form bimolecular crystals with this fullerene orientation. The orientation of the fullerene side groups within molecularly mixed polymer:fullerene phases should therefore be considered during the design of new fullerenes.

■ ASSOCIATED CONTENT

Ⓢ Supporting Information

A description of the materials, 2D GIXS patterns, a discussion of the energetics of PBTTT and PATBT, and an illustration of the two most common ICBA molecules intercalated between PBTTT side chains.This material is available free of charge via the Internet at http://pubs.acs.org.

■ AUTHOR INFORMATION

Corresponding Author

*E-mail: mmcgehee@stanford.edu

Notes

The authors declare no competing financial interest.

■ ACKNOWLEDGMENTS

This work is supported by the Department of Energy, Laboratory Directed Research and Development funding, under contract DE-AC02-76SF00515. The authors would like to acknowledge Eunkyung Cho, Chad Risko, and Jean-Luc Brédas from the Georgia Institute of Technology for fruitful discussions regarding the molecular structures. We would also

like to acknowledge Darin Laird of Plextronics, Martin Heeney and Iain McCullouch of Imperial College, and St-Jean Photochemicals for the synthesis and purification of the indene-C60 fullerenes, PBTTT polymers, and PCDTBT, respectively. Portions of this research were carried out at the Stanford Synchrotron Radiation Lightsource, a national user facility operated by Stanford University on behalf of the US Department of Energy, Office of Basic Energy Sciences.

REFERENCES

(1) Yu, G.; Gao, J.; Hummelen, J. C.; Wudl, F.; Heeger, A. J. *Science* **1995**, *270*, 1789−91.
(2) Brabec, C. J.; Gowrisanker, S.; Halls, J. J. M.; Laird, D.; Jia, S.; Williams, S. P. *Adv. Mater.* **2010**, *22* (34), 3839−3856.
(3) Carsten, D.; Vladimir, D. *Rep. Prog. Phys.* **2010**, *73* (9), 096401.
(4) Lenes, M.; Wetzelaer, G.-J. A. H.; Kooistra, F. B.; Veenstra, S. C.; Hummelen, J. C.; Blom, P. W. M. *Adv. Mater.* **2008**, *20* (11), 2116−2119.
(5) He, Y.; Li, Y. *Phys. Chem. Chem. Phys.* **2011**, *13* (6), 1970−1983.
(6) Lenes, M.; Shelton, S. W.; Sieval, A. B.; Kronholm, D. F.; Hummelen, J. C.; Blom, P. W. M. *Adv. Funct. Mater.* **2009**, *19* (18), 3002−3007.
(7) Choi, J. H.; Son, K.-I.; Kim, T.; Kim, K.; Ohkubo, K.; Fukuzumi, S. *J. Mater. Chem.* **2010**, *20* (3), 475−482.
(8) Frost, J. M.; Faist, M. A.; Nelson, J. *Adv. Mater.* **2010**, *22* (43), 4881−4884.
(9) Faist, M. A.; Keivanidis, P. E.; Foster, S.; Wöbkenberg, P. H.; Anthopoulos, T. D.; Bradley, D. D. C.; Durrant, J. R.; Nelson, J. *J. Polym. Sci., Part B: Polym. Phys.* **2011**, *49* (1), 45−51.
(10) Laird, D. W.; Stegamat, R.; Daadi, M.; Richter, H.; Vejins, V.; Scott, L.; Lada, T. A. Organic Photovoltaic Devices Comprising Fullerenes and Derivatives Thereof. U.S. Patent no. 2010/0132782, June 3, 2010.
(11) Zhao, G.; He, Y.; Li, Y. *Adv. Mater.* **2010**, *22* (39), 4355−4358.
(12) He, Y.; Chen, H.-Y.; Hou, J.; Li, Y. *J. Am. Chem. Soc.* **2010**, *132* (4), 1377−1382.
(13) Darin Laird, P. Plextronics, Inc.: Pittsburgh, PA. *Personal Communication*, 2011.
(14) Mayer, A. C.; Toney, M. F.; Scully, S. R.; Rivnay, J.; Brabec, C. J.; Scharber, M.; Koppe, M.; Heeney, M.; McCulloch, I.; McGehee, M. D. *Adv. Funct. Mater.* **2009**, *19* (8), 1173−1179.
(15) Cates, N. C.; Gysel, R.; Beiley, Z.; Miller, C. E.; Toney, M. F.; Heeney, M.; McCulloch, I.; McGehee, M. D. *Nano Lett.* **2009**, *9* (12), 4153−4157.
(16) Miller, N. C.; Gysel, R.; Miller, C. E.; Verploegen, E.; Beiley, Z.; Heeney, M.; McCulloch, I.; Bao, Z.; Toney, M. F.; McGehee, M. D. *J. Polym. Sci., Part B: Polym. Phys.* **2011**, *49* (7), 499−503.
(17) Miller, N. C.; Cho, E.; Junk, M. J. N.; Gysel, R.Risko, C.; Kim, D.; Sweetnam, S.; Miller, C. E.; Richter, L. J.; Kline, R. J.; Heeney, M.; McCulloch, I.; Acevedo, D.; Knox, C.; Hansen, M. R.; Dudenko, D.; Ammassian, A.; Chmelka, B. E.; Toney, M. F.; Brédas, J.-L.; McGehee, M. D. in progress.
(18) Savenije, T. J.; Grzegorczyk, W. J.; Heeney, M.; Tierney, S.; McCulloch, I.; Siebbeles, L. D. A. *J. Phys. Chem. C* **2010**, *114* (35), 15116−15120.
(19) Rance, W. L.; Ferguson, A. J.; McCarthy-Ward, T.; Heeney, M.; Ginley, D. S.; Olson, D. C.; Rumbles, G.; Kopidakis, N. *ACS Nano* **2011**, *5* (7), 5635−5646.
(20) Beiley, Z. M.; Hoke, E. T.; Noriega, R.; Dacuña, J.; Burkhard, G. F.; Bartelt, J. A.; Salleo, A.; Toney, M. F.; McGehee, M. D. *Adv. Energy Mater.* **2011**, *1* (5), 954−962.
(21) Wise, A. J.; Precit, M. R.; Papp, A. M.; Grey, J. K. *ACS Appl. Mater. Interfaces* **2011**, *3* (8), 3011−3019.
(22) Biniek, L.; Fall, S.; Chochos, C. L.; Anokhin, D. V.; Ivanov, D. A.; Leclerc, N.; Lévêque, P.; Heiser, T. *Macromolecules* **2010**, *43* (23), 9779−9786.
(23) Cates, N. C.; Gysel, R.; Dahl, J. E. P.; Sellinger, A.; McGehee, M. D. *Chem. Mater.* **2010**, *22* (11), 3543−3548.
(24) Miller, N. C.; Cho, E.; Gysel, R.; Risko, C.; Miller, C. E.; Sellinger, A.; Heeney, M.; McCullouch, I.; Brédas, J.-L.; Toney, M. F.; McGehee, M. D. in progress.
(25) Hirsch, A.; Lamparth, I.; Karfunkel, H. R. *Angew. Chem., Int. Ed. Engl.* **1994**, *33* (4), 437−438.
(26) Baumann, A.; Savenije, T. J.; Murthy, D. H. K.; Heeney, M.; Dyakonov, V.; Deibel, C. *Adv. Funct. Mater.* **2011**, *21* (9), 1687−1692.
(27) Azimi, H.; Senes, A.; Scharber, M. C.; Hingerl, K.; Brabec, C. J. *Adv. Energy Mater.* **2011**, *1* (6), 1162−1168.
(28) Jamieson, F. C.; Domingo, E. B.; McCarthy-Ward, T.; Heeney, M.; Stingelin, N.; Durrant, J. R. *Chem. Sci.* **2012**, *3*, 485−492, DOI: 10.1039/C1SC00674F.
(29) Riedel, I.; von Hauff, E.; Parisi, J.; Martín, N.; Giacalone, F.; Dyakonov, V. *Adv. Funct. Mater.* **2005**, *15* (12), 1979−1987.
(30) Shoaee, S.; Clarke, T. M.; Huang, C.; Barlow, S.; Marder, S. R.; Heeney, M.; McCulloch, I.; Durrant, J. R. *J. Am. Chem. Soc.* **2010**, *132* (37), 12919−12926.
(31) Dyer-Smith, C.; Reynolds, L. X.; Bruno, A.; Bradley, D. D. C.; Haque, S. A.; Nelson, J. *Adv. Funct. Mater.* **2010**, *20* (16), 2701−2708.
(32) Veldman, D.; Meskers, S. C. J.; Janssen, R. A. J. *Adv. Funct. Mater.* **2009**, *19* (12), 1939−1948.